Journal of Geomatics Vol 8 No. 2 October 2014

Image quality assessment of RISAT-1 SAR using trihedral corner reflectors in different beams

Maneesha Gupta, Anuja Sharma and B. Kartikeyan
Image Analysis and Quality Evaluation Division, SPDCG, SIPA, SAC, ISRO
Jodhpur Tekra, Ahmedabad-380 015, Gujarat- India
Email: maneesha@sac.isro.gov.in; anuja@sac.isro.gov.in; bkartik@sac.isro.gov.in

(Received: May 23, 2014; in final form: Sep 19, 2014)

Abstract: RISAT-1 is a C-band Synthetic Aperture Radar (SAR) satellite having unique capability of imaging the Earth using multiple beams (60 beams on either side), modes and polarizations and is the first SAR mission to realize circular polarimetry from space. Calibration and monitoring of SAR instrument parameters with respect to different beams and polarizations is required to ensure the consistency in the derived backscatter values. Use of passive corner reflectors as point targets is one of the fundamental approaches for SAR calibration. Here, by using trihedral corner reflectors as point sources, we measure the impulse response of these reflectors in the SAR image in both elevation and azimuth directions to evaluate the image quality parameters. The image quality parameters evaluated are Background to Peak (BP) ratio, spatial resolution in azimuth and range directions, Peak Side Lobe Ratio (PSLR), Integrated Side Lobe Ratio (ISLR) for each of the corner reflectors. The quality parameters are analysed, within the same scene having multiple corner reflectors in different beams on multiple dates, to evaluate the consistency of the system. Absolute calibration has been carried out by measuring the observed Radar Cross Section (RCS) and comparing it with the theoretical RCS. The products used for evaluation are Level-1 Single Look Complex and Ground Range in Fine Resolution Stripmap (FRS-1) mode, in circular, HH and VV polarizations. Results of the analysis show consistency for the deployed corner reflectors with a typical value of PSLR and ISLR in azimuth as -24 dB and -18 dB respectively and in range as -19 dB and -15 dB respectively. Geometric resolution in azimuth and slant range direction is found to be around 3.5 meters and 2.24 meters respectively, which are as per defined resolutions specifications for FRS SAR mode.

Keywords: RISAT-1, SAR, Corner reflectors, Point targets, ISLR, PSLR, BP ratio, RCS, FRS-1

1. Introduction

Remote sensing with active microwave instrument is becoming a norm of the day in operations for resource monitoring and other important applications, due to its day-night and all weather monitoring capability, as it utilizes its own source to illuminate the earth surface. Furthermore, being microwave, it is relatively free from atmospheric disturbances so accurate quantitative modelling is possible for different applications. Synthetic Aperture Radar (SAR) is one such active microwave instrument, which is used to measure the electromagnetic signal backscattered from the illuminated terrain. The essential parameter derived from SAR data is backscattering coefficient, which is a function of target properties, incidence angle and polarization (Ulaby et al., 1981). RISAT-1 is the first Indian space-borne SAR mission operating in C-band and having micro-strip phased array antenna with electronic beam steering capability which offers wide range of swaths and resolutions. Further, it supports quad and circular-polarization modes apart from usual co-polarization modes enabling a wide range of applications. Figure 1 gives the overview of RISAT-1 SAR modes (Anon., 2009) and Table-1 gives its detailed specifications.

Calibration and monitoring of SAR instrument parameters with respect to different beams and polarizations is required to ensure consistency in the derived backscatter values. This is addressed through different activities or processes, viz. onboard-calibration of individual Transmit Receive Modules (TRM) elements for gain and phase; monitoring raw signal data for signal mean bias, power imbalance, phase imbalance, Doppler centroid (Gupta et al., 2012; Amala et al., 2013 and Gupta et al., 2014), imaging over extended target like Amazon rain forest and its analysis for antenna-pattern and backscatter (Sharma et al., 2013), and Corner Reflector (CR) based analysis for geometric and radiometric calibration, the last one being the subject of this paper.

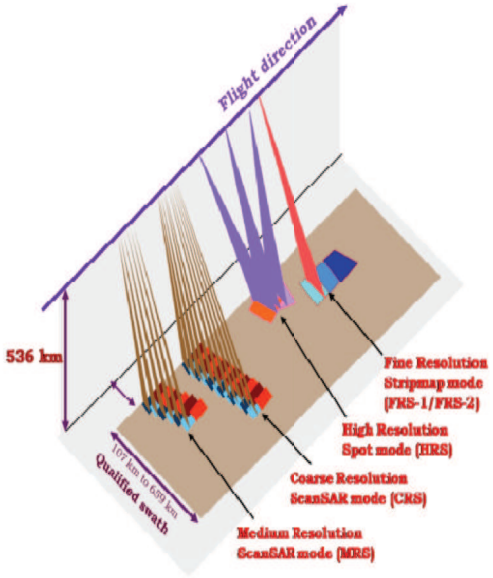

Figure 1: RISAT-1 SAR modes overview

Suitable corner reflectors of known properties are designed and deployed with proper alignment as imaging targets, which act as point sources in the SAR image (Skolnik, 1990). The impulse response function (IRF) is the point target return which measures the focusing and energy distribution in SAR image in both elevation and azimuth directions. Impulse response measurements on such targets in SAR data is similar to the Point Spread Function (PSF) derivation performed for optical imagery. Point target response measurement is useful to measure geometric aspects like resolution and absolute calibration by evaluating Radar Cross Section (RCS) of the target (Martinez and Marchand, 1993)

Table 1: RISAT-1 SAR specifications

Imaging Modes		***HRS/ C-HRS**	***FRS-1/C-FRS-1**	***FRS-2/C-FRS-2**	***MRS/C-MRS**	***CRS/C-CRS**
Applicable Polarization combinations		Single or dual/circular		Quad/circular	Single or dual/circular	
Swath /Spot (km)	**Defined**	10 (Az.) x 10 (Rng.)	25	25	115	223
	Experimental	100 (Az.) x 10 (Rng.)	---	---	---	---
Resolution (Az x slant range)		1m x 0.7 m	3m x 2m	9m x 4m	21-23m x 8m	41-55 m x 8m
Minimum sigma naught (dB) (Qualified Region)		-16.3	-17	-18	-18	-18

*HRS- High resolution stripmap; FRS- Fine Resolution stripmap; MRS Medium Resolution ScanSAR; CRS coarse resolution ScanSAR; C-FRS, C-MRS, C-HRS, C-CRS refers to circular polarization in respective modes

Before the launch of ERS-1, Freeman (1992) reviewed the SAR calibration and image quality assessment based on IRF using both complex and square law detected (single look and multi-look) images and found the parameters, which affects the degree of coherence in SAR images and in turn the IRF. In ENVISAT-ASAR, during commissioning phase, the image quality was assessed similarly, as in ERS-1 and 2 using four ESA transponders deployed within the Netherlands , the four RADARSAT transponders located within Canada and the German national ground station (Closa and Rosich, 2001). Results showed an important finding in terms of azimuth and range sampling where Peak Side Lobe Ratio (PSLR) and Integrated Side Lobe Ratio (ISLR) were falling outside the expected range due to the under-sampling in precision image product (Meadows and Wright, 2002). Donald et al. (2001) also studied the applicability of corner reflectors for geometric corrections using RADARSAT Fine Mode SAR data. Corner reflector and transponders were also used to check the registration between the different polarizations and frequency images by measuring the interpolated peak positions (Freeman and Curlander, 1989).

During the initial phase of RISAT-1 SAR, a number of CRs were deployed at four different sites near Ahmedabad and Hyderabad (Prakash et al., 2012). In this paper, the consistency of derived calibration and performance parameters have been evaluated and analysed using the CR response with respect to different beams and dates. The CRs response analysis is carried in co-polarization and circular polarization images i.e. in RH (right hand circularly polarised transmit and linearly receive in Horizontal polarization), HH (Horizontal transmit, horizontal receive), RV (right hand circularly polarised transmit and linearly receive in Vertical polarization) VV (Vertical transmit, Vertical receive). Point target analysis for HV and VH is not carried out in the present work due to weak return energy from the corner reflectors, as the type of corner reflectors (trihedral) deployed are effective for co-polarization and circular polarization channels only. Section 2 of this paper describes the specific methodology and approach used for the computation of IRF parameters. Section 3 gives the details of the deployment sites, corner reflectors and SAR data products used for analysis. Analysis and evaluation results are discussed in Section 4 followed by the concluding remarks in section 5 based on various factors, on which the response of CR depends i.e. accuracy of CR alignment with respect to antenna beam, homogeneity of the deployment site, background quality in terms of clutter on one hand and system and processing parameters on the other hand.

2. Methodology and approach

The analysis of the signature of a point target in SAR image allows the determination of several parameters related to SAR spatial resolution and the presence of undesired, but inevitable, side lobe peaks (Gray et al., 1990). The main response is characterized by the half power widths of the peak response in the along and the cross track directions, and rest are the side lobe and integrated side lobe levels. For absolute calibration, point target RCS is computed and compared with the theoretical RCS of CR. Different approaches to evaluate IRF parameters are available in literature (Lu and Sun, 2007; Sanchez, 1991; Franceschetti et al., 1991; Guignard, 1979; Holm et al., 1991; Anon., 1990 and 1991), especially the ISLR with differences in the adoption of the areas in which the energy is integrated. The approach adopted here is based on ESA's approach (Anon. 1990 and 1991; Mehta et al., 2011) with few modifications discussed in the next paragraph. Similarly, for RCS computation, two methods are discussed (Gray et al., 1990) viz. peak method and the integration method on pixel value. Integral method, which is independent of processor gains and focus, is adopted in this analysis.

Computation of IRF and derived parameters should ideally be taken over a flat homogeneous background so as to minimize the background noise. The steps followed for background corrected image using corner reflectors as point target, is given below (Gupta et al., 2013):-

- Select a chip of n x n pixels around the corner reflector (say n = 16) as amplitude image of 256 pixels.
- Convert the amplitude image in to pixel intensity image

$$P_i = DN_i^2 \quad (1)$$

- Select four corner windows to compute average background intensity value of each of the four windows as clutter as shown in Figure 2. (In this analysis, 5 × 5 window is selected)
- Computing the average background intensity value <*B*>

$$< B > = \frac{1}{N_b} \sum_1^{N_b} DN_i^2 \quad (2)$$

where, N_b is the number of pixels in corner window and DN_i is the amplitude of i^{th} pixel in window.

- Correction for background contribution to get background corrected intensity image of the chip around the point target. Mathematically, Background corrected power image is given as

$$P_c = P_i - <B> \quad (3)$$

- Interpolating the background corrected intensity image by a factor f (say f= 16) to get IRF in range and azimuth direction such that N = n × f (16×16 =256)
- Calculate the peak value from this zoomed chip
- Extract samples in range and azimuth centred on the peak for IRF.

Calculation of resolution and IRF parameters from this power corrected image

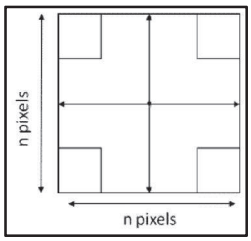

Figure 2: Chip around the point target for removing background clutter

Detailed formulation for evaluating each parameter is given as follows.

2.1. Background to Peak (BP) ratio: Background to Peak ratio is defined as the ratio of Average energy of the background to peak power. Mathematically, Background to peak (BP) ratio in dB is computed as:

$$\text{BP ratio} = 10 \times \log_{10} \left(\frac{<B>}{DN_i^2}\right) \text{(dB)} \quad (4)$$

Where, <*B*> is the average background intensity and DN_i^2 is the intensity of the peak.

2.2. Impulse Response Function: IRF of the point target and the derived quality parameters in Range/Azimuth directions are-

2.2.1. 3dB Impulse response beam width: It is defined as the width of the main lobe at a power level 3 dB down from the peak. It gives the measure of geometric (spatial) resolution in both azimuth and range directions in pixels. In general, resolution is higher than the pixel/line spacing. Using line and pixel spacing, the resolution can be converted to meters.

2.2.2. Left and Right Side Lobe Ratio (LSLR/RSLR): A side lobe occurring to the first right side of the most intense peak of the IRF below 3dB is known as right side lobe. Similarly, side lobe to the left of the most intense peak of the IRF below 3dB forms the left side lobe and the corresponding ratio of these side lobe peaks with the main lobe peak constitutes the right side lobe ratio and the left side lobe ratio respectively and is computed in both range and azimuth directions.

$$\text{LSLR} = 10 \times \log_{10}\left(\frac{DN_{flsl}^2}{DN_{ml}^2}\right) \text{(dB)} \quad (5)$$

Where, DN_{flsl}^2 is the peak intensity of the first left side lobe and DN_{ml}^2 is the intensity of the peak of the main lobe. Similarly, Right side lobe is calculated as per equation 5, replacing DN_{flsl}^2 with DN_{frsl}^2 as the peak intensity of the first right side lobe.

2.2.3. Peak Side Lobe Ratio (PSLR): It describes the power resolution between the main lobe and side lobe and is defined as the ratio of the intensity of the most intense peak of the IRF outside a rectangle of 2×2 resolution lengths and within a rectangle of 10×10 resolution lengths to the peak intensity in the main lobe (i.e. within a rectangle of 2×2 resolution lengths).

$$\text{PSLR} = 10 \times \log_{10}\left(\frac{DN_{sl}^2}{DN_{ml}^2}\right) \text{(dB)} \quad (6)$$

Where, DN_{sl}^2 is the intensity of the most intense peak between 2×2 and10×10 resolution lengths and DN_{ml}^2 is the intensity of the peak of the main lobe.

2.2.4. Integrated Side Lobe Ratio (ISLR): It describes the extent to which energy is spread around the main lobe and is defined as the ratio of the integrated energy in the side lobe region of the two dimensional (range and azimuth) IRF relative to the integrated energy in the main lobe region. Since the time of ERS-1 there are various approaches to compute ISLR (Martinez and Marchand, 1993; Lu and Sun, 2007; Sanchez, 1991; Franceschetti et al. 1991; Guignard 1979; Holm et al., 1991; Anon. 1990 and 1991). In the present work, ISLR is computed as:

$$\text{ISLR} = 10 \log_{10}\left(\frac{E_1}{E_2 - E_1}\right) \text{(dB)} \quad (7)$$

Where E_1 is the energy enclosed within two times of 3dB resolution width and E_2 is the energy enclosed within 20 times of 3dB resolution width excluding the main lobe or two times the 3dB resolution width.

2.3. Radar Cross-Section (RCS): In general, the efficiency of the terrain to reflect the radar pulse is termed as the "radar cross section".

2.3.1. Observed RCS (σ)

The expression to calculate the RCS (σ) of a point target from RISAT-1 SAR Level-1 imagery is:

$$\sigma = 10 \times \log_{10} \sum_i^k \sum_j^l DN_{ij}^2 + 10 \times \log_{10}(PT_a) - K + 10 \times \log 10 \left(\frac{\sin i_{pt}}{\sin i_{ref}}\right) (dBm^2) \quad (8)$$

where, $\sum_i^k \sum_j^l DN_{ij}^2$ is the back ground corrected point target power with i, j, k and l are defined by the window around the point target, PT_a is the point target area and is defined as line spacing × pixel spacing, i_{pt} is the incidence angle at point target and i_{ref} is the incidence angle at scene centre and K is the calibration constant from the meta file of the data product.

2.3.2. Theoretical RCS of trihedral corner reflectors

i. Triangular Trihedral (TT) $\sigma_{TT}^{tri} = \frac{4\pi a^4}{3\lambda^2}$

ii. Square Trihedral (ST) $\sigma_{ST}^{tri} = \frac{12\pi a^4}{\lambda^2}$

iii. Circular Trihedral (CT) $\sigma_{CT}^{tri} = \frac{4.97\pi a^4}{\lambda^2}$

where, a is the leg length of the trihedral and λ is the RADAR wavelength

These parameters have been studied using semiautomatic software RISAT-1 Point Target ANalysis (RI-PTAN) designed and developed (Prakash et al., 2012) for the visualization and identification of corner reflector from the SAR image. The software facilitates to graphically analyze the impulse response profiles in azimuth and range direction. The profiles can also be visualized as contour and surface plot for the selected corner reflector. The RI-PTAN software tool has following salient features:

- Extraction of image files and meta information from the CEOS formatted Level-1 products
- Display of overview and full resolution amplitude image for the selected polarization. The full resolution image can be enhanced and zoomed to make CR clearly visible in the image.
- Option is given in Graphic User Interface (GUI) to select the CR type and shape.
- Once the CR is identified, the PSLR, ISLR, geometric resolution are automatically computed from the zoomed profiles.
- The geo-location (latitude and longitude) of the target is computed using the grid associated with the product. Unique target ID is associated with every point target based on its serial number, beam and polarization.
- The software has the capability to identify and analyze the natural point targets in addition to the deployed corner reflectors.
- The software has a built-in data visualization package for displaying the IRF in various forms for better interpretation of the energy distribution as shown in Figure 3. The zoomed 1D profile provides a cross-sectional view in azimuth and range direction and scaled 2-D intensity image provides the top-view of the target whereas the power contour map and 3-D surface plot (see Figure 4) gives the energy level concentrated in the main lobe.

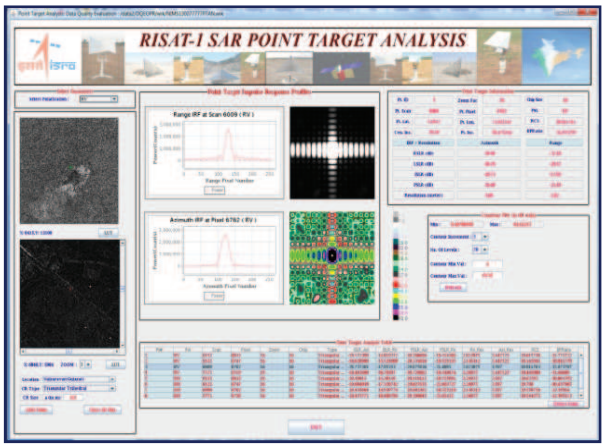

Figure 3: Snap shot of the Graphical User Interface (GUI) of the software tool RI-PTAN, showing 1D impulse response, its 2D intensity image and contour map, computed on a scene carrying corner reflector

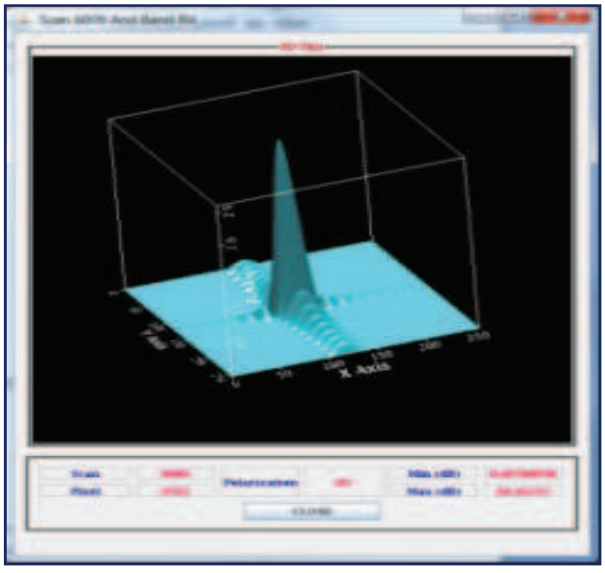

Figure 4: 3D view of the IRF, with details of energy distribution in the resolution cell.

3. Corner reflectors deployment and data description

Calibration using corner reflectors is one of the reliable means to perform radiometric, geometric, and impulse

response measurements for satellite-based SAR instruments. It has certain advantages like low maintenance and low cost compared to active devices such as transponders. For the point target analysis, passive corner reflectors of known radar cross section are deployed considering three important points (i) orientation of corner reflector (CR) with respect to SAR antenna (ii) the deployment site characteristics and (iii) size and material of the CR i.e it should have sufficient energy for scattering. Precise deployment of CR is the primary requirement and for best results, CR should be pointed directly along the bore sight of the SAR antenna (Norris et al., 2004). Secondly, deployment sites should be free from the multi-path contributions and should be located distant from the power lines and housing colonies (Donald et al., 2001).

In view of this, since launch of RISAT-1 SAR, calibration teams of ISRO deployed passive corner reflectors at five different sites in India - Space Applications Centre (Ahmedabad), Near Space Applications Centre Bopal campus (Ahmedabad), Nalsarovar (Near Ahmedabad), Shadnagar-NRSC (Hyderabad) and Narkhoda (Hyderabad) as shown in Figure 5. The CRs deployed are basically, the trihedral corner reflectors of different sizes and shapes (triangular, square and circular) as shown in Figure 6 having RCS in the range 24.87 dBm^2 to 35.79 dBm^2. Deployments of corner reflectors were made in a way, to characterize different beams at varying incidence and look angles, in available polarization. Detailed specifications of the corner reflectors are defined in Table 2 and 3 with respect to RV/VV and RH/HH polarization respectively.

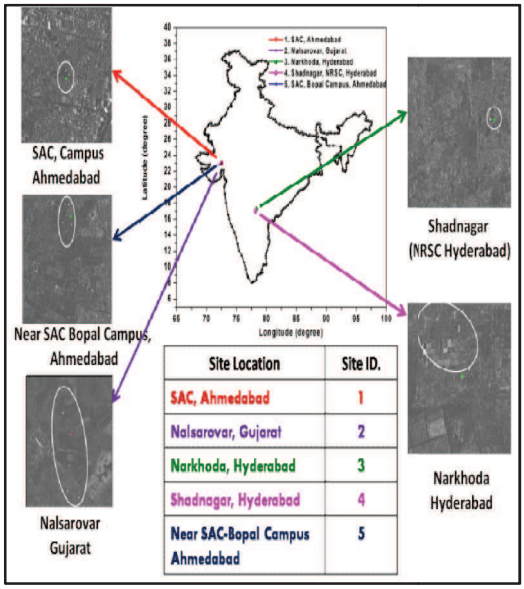

Figure 5: Calibration site view (Full Map) and SAR image view (Map source: National Data Centre (NDC)- National Remote Sensing Centre -(NRSC) Hyderabad)

Figure 6: Trihedral corner reflectors used for calibration analysis (a) Square trihedral of size 75cm (b) Triangular trihedral of size 90cm. (source: NRSC (Hyderabad); SAC(Ahmedabad))

Table 2: Corner reflector deployment details in RV/VV polarization

S. No	Site Id*	**CR Type	Size (cm)	Pol	Theoretical RCS dBm^2	Incidence angle	CR Ref No
1	1	TT	90	RV	29.43	43.35	CR1
2	1	TT	90	RV	29.43	43.34	CR2
3	1	TT	90	RV	29.43	43.34	CR3
4	2	TT	90	RV	29.43	50.18	CR4
5	2	TT	90	RV	29.43	50.18	CR5
6	2	TT	90	RV	29.43	50.17	CR6
7	2	TT	90	RV	29.43	50.17	CR7
8	3	ST	75	RV	35.79	43.68	CR8
9	3	ST	75	RV	35.79	43.67	CR9
10	3	ST	75	RV	35.79	43.64	CR10
11	4	ST	75	RV	35.79	26.9	CR11
12	4	ST	40	RV	24.87	26.91	CR12
13	4	ST	40	RV	24.87	26.91	CR13
14	3	ST	75	VV	35.79	29.41	CR14
15	3	ST	75	VV	35.79	29.39	CR15
16	3	ST	75	VV	35.79	29.36	CR16

*Site Id Definition is given in Figure5, **CR- Corner Reflector, TT- Triangular Trihedral, ST- square trihedral, CT- circular trihedral

Table 3: Corner reflector deployment details in RH/HH polarization

S. No	Site Id*	**CR Type	Size (cm)	Pol.	Theoretical RCS dBm^2	Incidence Angle	CR Ref No
1	1	TT	90	RH	29.43	43.35	CR1
2	1	TT	90	RH	29.43	43.34	CR2
3	1	TT	90	RH	29.43	43.34	CR3
4	2	TT	90	RH	29.43	50.18	CR4
5	2	TT	90	RH	29.43	50.17	CR5
6	2	TT	90	RH	29.43	50.18	CR6
7	2	TT	90	RH	29.43	50.17	CR7
8	3	ST	75	RH	35.79	43.68	CR8
9	3	ST	75	RH	35.79	43.67	CR9
10	3	ST	75	RH	35.79	43.64	CR10
11	4	ST	75	RH	35.79	26.9	CR11
12	4	ST	40	RH	24.87	26.91	CR12
13	4	ST	40	RH	24.87	26.91	CR13
14	1	TT	90	HH	29.43	37.9	CR14
15	1	TT	90	HH	29.43	37.9	CR15
16	1	TT	90	HH	29.43	37.9	CR16
17	5	TT	90	HH	29.43	38.27	CR17
18	5	ST	60	HH	31.93	38.27	CR18
19	5	ST	60	HH	31.93	38.28	CR19
20	5	CT	60	HH	28.09	38.28	CR20
21	5	TT	90	HH	29.43	38.28	CR21

*Site Id Definition is given in Figure 5 **CR- Corner Reflector, TT- Triangular Trihedral, ST- square trihedral, CT- circular trihedral

In the present work, Image quality parameters are monitored and evaluated from SAR Level-1 Single Look Complex (SLC) and Ground Range (GR) products for the scenes carrying CR based point targets. RISAT-1 SAR products are available in standard CEOS format. The Level-1 SLC product is generated after range and azimuth compression of SAR raw signal data. Further, Level-1 GR multi-look product is obtained by ground projection. Image Geo-location grid is available with data product is used for locating the features on ground (Mehra et al., 2013).

The scenes acquired over the calibration sites are available in circular, VV+VH and HH+HV polarization covering different beams in FRS-1 mode whose defined resolution is 3m in azimuth and 2m in range direction. Details of SAR images used here for analysis are given in Table 4. Samples of typical detected images in slant range and GR with full resolution are shown in Figure 7 where the overview image is of size 25×25 km (FRS-1 mode; no north aligning) with its full resolution image of size 256×256 pixels. One image is in slant range and other is in GR therefore scale is variable.

Table 4: Details of Level-1 SLC and GR image acquisition for point target analysis

*Site Id	DOP	Imaging Node	Beam No/#Look Dir.	Polarization
1	16th May 2012	Ascending	38/R	RV+RH
2	6th June 2012	Descending	114/L	RV+RH
3	17th June 2012	Descending	38/R	RV+RH
4	18th June 2012	Descending	16/R	RV+RH
4	24th May 2012	Descending	19/R	VV +VH**
5	2nd Feb 2013	Ascending	30/R	HV**+HH

**Site Id Definition is given in Figure 5;* ** Point target analysis for VH and HV is not carried out in the present work due to weak return energy; #R-Right look L-Left look

4. Analysis and results

A systematic analysis has been carried out for the RISAT-1 SAR image quality performance on six scenes covered in different SAR-beams (look angle) in FRS-1 mode by characterizing the IRF using passive corner reflectors as point targets. As described in Section 2, before the computation of IRF, background correction is required to assure that the radar backscatter is wholly coming from the corner reflector. The background may introduce noise in the return which can be analyzed from background to peak ratio. This is calculated for each point target of the scene using an appropriate window of 5×5 pixels leaving the maximum intensity pixel and the side lobes in azimuth/range direction. Variation in BP ratio is tabulated in Table 5, showing the acceptable limits of BP Ratio which is better than -28 dB for Level-1 SLC products and -20dB for GR products

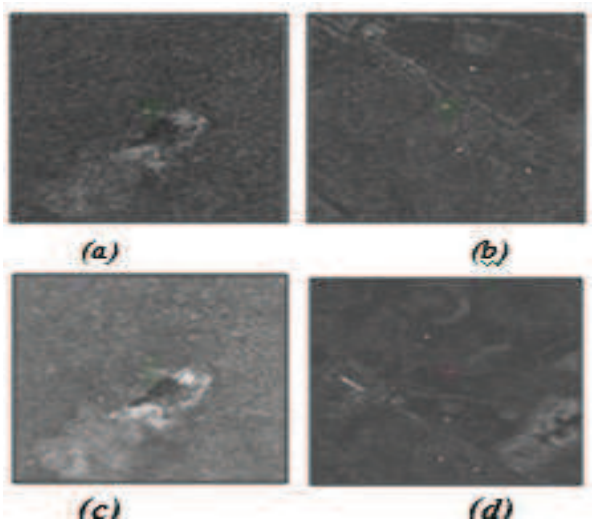

Figure 7: Detected image of Nalsarover calibration site (a)Level-1 SLC image Overview (25×25 km) (b)Full resolution showing CRs in Level-1 SLC image (1:1 scale with 256×256 pixels), (c)Ground Range (GR) image overview (25×25 km) (d)Full resolution, showing CRs in GR image. (1:1 scale with 256×256 pixels).

Table 5: Variation of Background to Peak (BP) Ratio

Parameter	Polarization	Level-1 SLC	Level-1 GR
Background to Peak Ratio (dB)	RV/VV	-33.36 to -22.45	-25.86 to -13.86
	RH/HH	-32.97 to -20.49	-24.96 to -9.62

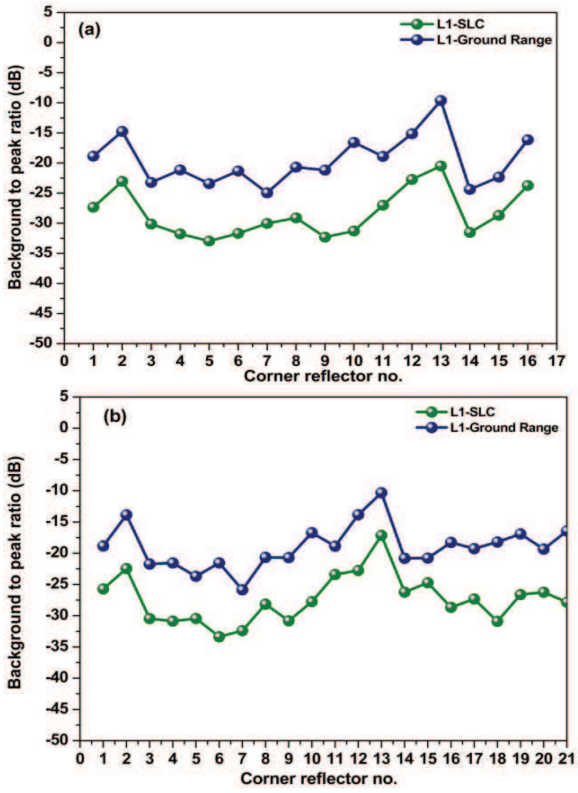

Figure 8: Background to peak ratio in Level-1 SLC and GR data for (a) RV/VV (b) RH/HH polarization
*(*CR numbering as per Table 2 and 3)*

From the plots of background to peak ratio (Figure 8 a, b) it is observed that CR-2 (SAC Ahmedabad, TT of size 90 cm) and CR-13 (Shadnagar, ST of size 40 cm) corner reflectors show a high BP ratio in both polarizations, suggesting the contribution of background noise in the backscatter from the reflector. The remaining corner reflector background seems to be homogeneous and is within the acceptable limits. The background noise which generally affects the main lobe and side lobes of the response function needs to be subtracted. The average background noise computed is subtracted using the methodology described in Section 2, before further computations of IRF quality parameters and the radar cross section. The radar cross sections are computed from both Level-1 SLC and GR products and results are summarized in Table 6.

Table 6: Theoretical and Mean Observed RCS in SLC and GR Images

CR Type	Size (cm)	Theoretical RCS (dBm^2)	Observed RCS (dBm2)			
			RV/VV		RH/HH	
			Level-1 SLC	Level-1 GR	Level-1 SLC	Level-1 GR
Triangular Trihedral	90	29.43	29.11	28.49	29.03	28.45
Square Trihedral	75	35.79	34.42	34.18	31.88	31.96
Square Trihedral	40	24.87	20.74	22.1	19.37	20.65
Square Trihedral	60	31.93	NA*	NA*	30.58	28.58
Circular Trihedral	60	28.09	NA*	NA*	28	27.33

NA* : RCS not available as corner reflector not seen in the image

From Figure 9 (a) and (b) it is seen that the observed RCS for the Nalsarovar and SAC main campus deployed triangular trihedral (TT) corner reflectors of 90 cm size is matching well with the theoretical RCS except CR 2 with a difference of less than 0.5 dBm^2, suggesting a perfect deployment and background homogeneity. RCS of CR 2 is off from the theoretical RCS by 5.5 dBm^2 which might be due to the background noise or close deployment of CRs.

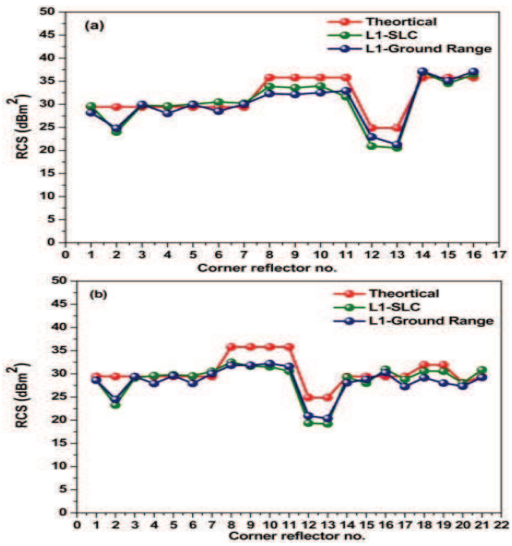

Figure 9: Theoretical and Observed RCS for Level-1 SLC and Ground range data in (a) RV/VV (b) RH/HH Polarization (*CR numbering as per Table 2 and 3)

The observed RCS for the square trihedral corner reflectors (75 and 40 cm) deployed at Shadnagar and Narkhoda is differing by nearly 4 dBm^2. This might be due to the improper alignment of corner reflector with the bore-sight or due to SAR processing. The backscatter from the square & circular trihedral of 60 cm is not mentioned for RV/VV image as these are not visible in this polarization as mentioned in Table 2 and 3. Also, the observed RCS in both Level-1 SLC and GR products are same, suggesting the preservation of peak intensity value during SAR processing. Further, from the background subtracted intensity image, resolution is calculated using the 3dB width of the IRF in both azimuth and range (slant range in SLC products and GR in Level-1 GR products) directions.

The geometric resolutions observed in both the products types for all the polarizations, matches well within the acceptable limits. In RISAT-1 FRS-1 mode, the expected azimuth resolution is 3.33m in SLC products and 13.33m in GR products for 4 azimuth looks. The expected slant range resolution is 2.34 m and GR resolution varies with incidence angle with minimum value of 4.38 m for 2 range looks. From the plots given in figures 10 and 11, the observed resolutions are in the satisfactory range. In SLC products the azimuth resolution lies between ~3m-4m except the corner reflectors 10, 14, 15, 16 & 21 seen in RH/HH image (Figure 10b) where the observed values are greater than 4m. However, in GR products the azimuth resolution is consistent and lies in range of 9.52 m to 10.92 m.

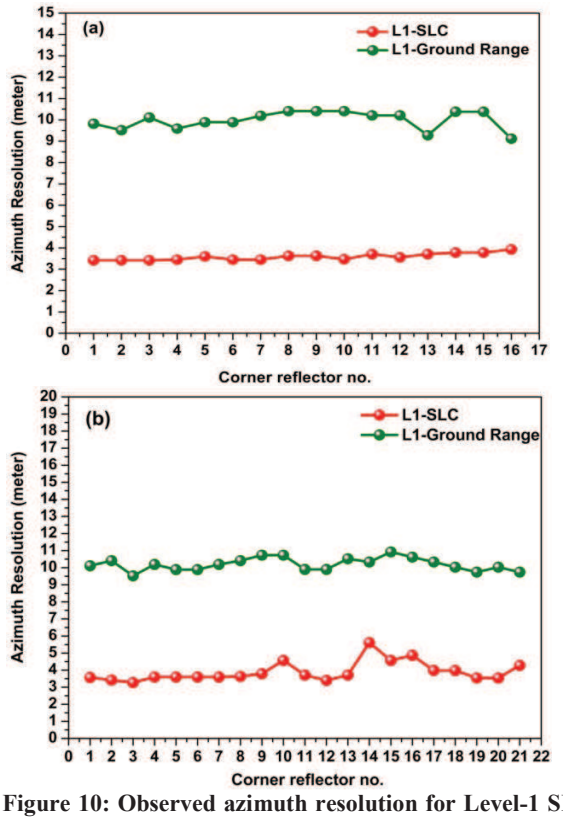

Figure 10: Observed azimuth resolution for Level-1 SLC and GR data in (a) RV/VV (b) RH/HH polarization (*CR numbering as per Table 2 and 3)

The range resolutions observed in SLC are consistent and are around 2.21 m. In case of GR products it varies from minimum 4.78 m to 12.38 m for different corner reflectors, which is as per expectation as GR resolution varies with local incidence angle.

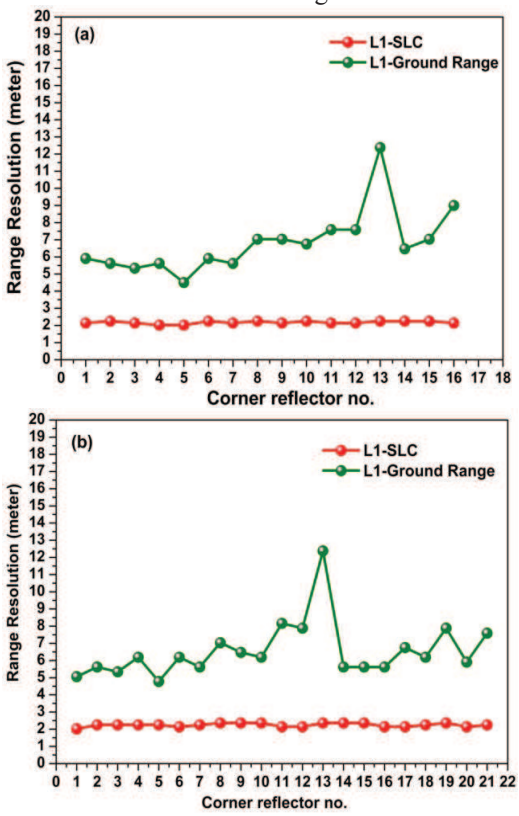

Figure 11: Observed range resolution for Level-1 SLC and GR data in (a) RV/VV (b) RH/HH polarization (*CR numbering as per Table 2 and 3)

Image quality using IRF in both product types were analysed from the zoomed intensity image, carrying corner reflector, after the background correction. Observed values are tabulated in Table 7. From the plot in figure 12 it is clear that statistically, fluctuation in peak side lobe ratio are observed in Shadnagar scene with square trihedral corner reflectors, which indicate poor energy return in main lobe with respect to side lobe from the identified CR in the scene which may affect the classification of features. PSLR in Range (Figure 12) is better than -18dB (SLC)/-15.5dB (GR) and in azimuth, it is better than -25 dB (SLC)/-19 dB (GR).

The energy spread around the main lobe is studied using integrated side lobe ratio of the 2D IRF, which is stable in both product types (Figure 13) and is better than -19dB (SLC)/-18dB (GR) in azimuth direction and in range, it is better than -15 dB (SLC)/-14dB (GR) which is as per expectations and can be interpreted that SAR processor is efficient in providing good contrast SAR images, with no loss of target detection. Also, for precisely understanding the energy distribution in the immediate side lobe in the backscatter return from a point target, Left and Right side lobe ratios were studied and the observed RSLR/LSLR in azimuth direction is better than -30dB (SLC)/-21dB (GR) and in range direction it is better than -23dB in both the product types.

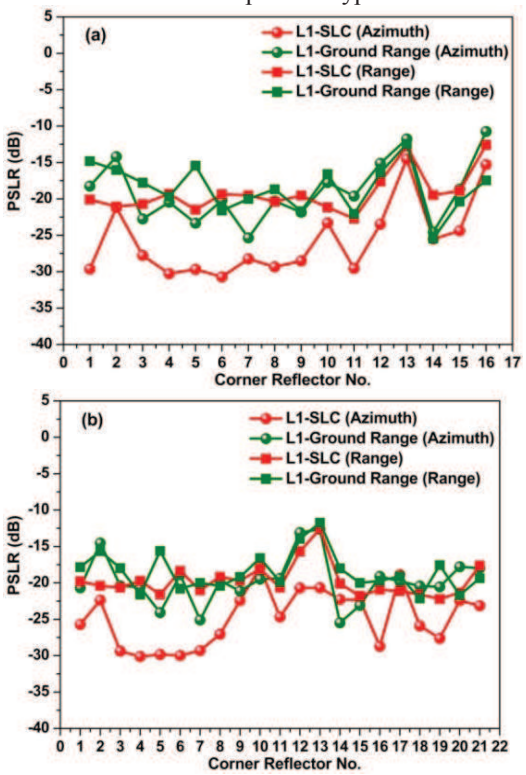

Figure 12: Observed PSLR for Level-1 SLC (shown in red) and GR (shown in green) data in azimuth (shown as dots) and range (shown as squares) directions in (a) RV/VV (b) RH/HH polarization (*CR numbering as per Table 2 and 3)

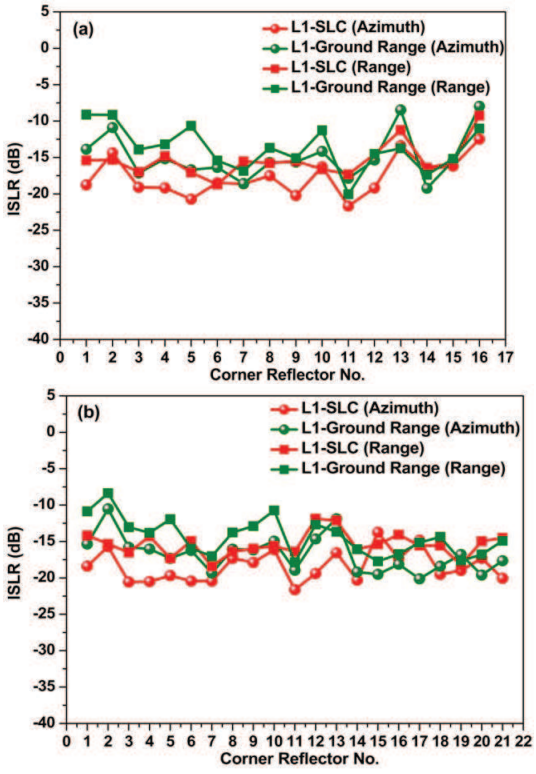

Figure 13: Observed ISLR for Level-1 SLC (shown in red) and GR (shown in green) data in azimuth (shown as dots) and range (shown as squares) directions in (a) RV/VV (b) RH/HH polarization (*CR numbering as per Table 2 and 3)

Table 7: Observed statistics of IRF quality parameters for SLC and GR images

IRF Parameters	Pol.	Total CR's	Level-1 - Single Look Complex					Level-1 -Ground Range				
			Expected Value	Mean	Std Dev	Min.	Max.	Expected Value	Mean	Std Dev	Min.	Max.
PSLR_#Azi. (dB)	RV/ VV	16	-20	-25.71	5.10	-30.72	-14.52	-20	-19.05	4.30	-25.36	-10.75
PSLR_@Rng.(dB)			-20	-17.67	2.61	-21.67	-12.49	-20	-14.90	3.26	-19.22	-7.97
ISLR_Azi. (dB)			-13	-19.16	2.79	-22.72	-12.59	-13	-18.53	3.30	-25.46	-12.44
ISLR_Rng. (dB)			-13	-15.39	2.28	-18.71	-9.26	-13	-13.76	3.01	-20.06	-9.11
Azi._Res. (m)			3.33	3.58	0.15	3.42	3.93	13.33	9.98	0.42	9.12	10.41
Rng_Res*. (m)			2.34	2.17	0.07	2.02	2.25	-	-	-	-	-
PSLR_Azi (dB)	RH/ HH	21	-20	-24.82	3.87	-30.11	-17.9	-20	-19.70	3.36	-25.48	-12.64
PSLR_Rng. (dB)			-20	-18.41	2.15	-21.62	-13.75	-20	-16.79	2.50	-20.13	-10.51
ISLR_Azi. (dB)			-13	-19.71	2.28	-22.21	-12.57	-13	-18.51	2.64	-22.14	-11.73
ISLR_Rng. (dB)			-13	-15.41	1.63	-18.41	-11.87	-13	-14.37	2.59	-17.87	-8.36
Azi._Res. (m)			3.33	3.89	0.57	3.27	5.61	13.33	10.19	0.37	9.52	10.92
Rng_Res*. (m)			2.34	2.24	0.10	2.02	2.36	-	-	-	-	-

*Range resolution for Level-1 -GR varies with local incidence angle; #Azi. –Azimuth;@Rng- Range

5. Conclusions

In this paper, image quality evaluation has been carried out systematically using trihedral corner reflectors of various shapes and sizes deployed at five different sites. Quantitative analysis was performed over the six scenes (Table 4) in different beams (4 left beams 38, 16, 19, 30 and one right beam 114) having trihedral corner reflectors in RISAT-1 fine resolution stripmap-1 mode imagery. BP ratio was observed better than -28dB suggesting a noise free signal from the scatterer. The observed RCS of the point target from the image matches with the theoretical RCS within ±1 dBm^2 except for the CRs (square trihedral) deployed over Shadnagar, where it overshoots up to $4dBm^2$. RCS study suggests that polarization independent triangular trihedral corner reflector of size 90cm or less is perfect for RISAT-1 SAR image quality analysis and calibration. The variation in RCS may be either due to particular corner reflector properties or due to its improper alignment. Statistical analysis over these reflectors shows an average standard deviation of 3.4dB in PSLR and 2.5dB in ISLR in range/azimuth direction and for both SLC and GR products, whereas resolution has a standard deviations of 0.08 in slant range, and 0.3 in azimuth. Results shows consistency in the quality parameter achieved from RISAT-1 SAR. In addition to these parameters, other data quality evaluation parameters such as location accuracy, radiometric stability and radiometric accuracy can also be evaluated using corner reflectors which require a fixed array of corner reflectors of similar type covering end to end swath in the same scene. Also, these measurements should be repeated periodically to monitor the temporal variations. Further, a continuous study using advanced approaches is required on SAR image quality assessment and calibration to achieve better quality products, in order to fulfil the user's requirements.

Acknowledgements

Authors are grateful to Padmashri A. S Kiran Kumar, Director, Space Applications Centre (SAC), Ahmedabad, for providing the motivation to carry out this work.

Further, authors would like to thank Shri Santanu Chowdhury, Deputy Director, Signal and Image Processing Area (SIPA), SAC and Shri. B. Gopala Krishna, Group Director, Satellite Photogrammetric and Digital Cartography Group, SIPA/SAC for their continued guidance. Special thanks are due to RISAT-1 project team at ISRO for their extensive efforts and support provided to us during the present work. Also, authors extend thanks to all the members of the Image Analysis and Quality Evaluation Division (IAQD) for their whole-hearted support.

References

Amala, V.M.S., M. Gupta, K. Selvavinayagam, B. Kartikeyan, S. Suresh Babu (2013). RISAT-1 SAR Level-0 raw data quality evaluation. International Journal of Earth Science and Engineering (IJEE), Vol.6 No. 01-(01),February 2013, pp. 1949-1954

Anonymus (1991). ESA, ECISAR test image: Quality analysis and calibrations measurements. er-tnepo-gp-1902, estec-esa ed., 1991.

Anonymus (1990). ESA, Technical note on the ECISAR test image, ER-TN-EPO-GP-1901, ESATECESA ed., 1990.

Anonymous (2009) RISAT-SAR Payload, DDR Document: SAC/RISAT/DDR/01/2009, Space Applications Centre, Ahmedabad.

Closa, J. and B. Rosich (2001). The ASAR ground processor verification activities. CEOS-SAR-01-056.

Donald, M. Ugsang, K. Honda and G. Saito (2001). Assessment of small passive corner reflectors for geometric correction of RADRASAT fine mode SAR data. 22nd Asian Conference on Remote Sensing, 5-9 November 2001, Singapore

Franceschetti, G., R. Lanari V. Pascazio and G. Schirinzi (1991). Wide angle SAR processors and their quality assessment. Geoscience and Remote Sensing Symposium, IGARSS '91, remote Sensing: Global Monitoring for Earth Management (Volume 1) pp. 287 – 290.

Freeman, A. (1992). SAR Calibration: An Overview. IEEE Trans. on Geoscience and Remote Sensing, vol. 30, No.6, page- 1107-1121.

Freeman, A. and J.C. Curlander (1989). Radiometric correction and calibration of SAR images. Photogrammetric Engineering & Remote Sensing, vol. 55, No. 9, pp. 1295-1301

Gray, A.L., P.W. Vachon, C.E. Livingstone, T.I. Lukowski (1990). Synthetic Aperture Radar calibration using reference reflectors. IEEE Tans. Geosci. Remote Sensing, vol. 28, No. 3, pp.224-240.

Guignard, J. (1979). Final acceptance of the MDA software SAR processor. In SEASAT SAR processor workshop, pp. 91 – 100, ESA SP-154, 1979.

Gupta M., S. Prakash, V. Malhotra, A. Sharma and B. Kartikeyan (2012). RISAT-1 SAR raw data quality evaluation and monitoring for stripmap mode using SAR-RQuEST, International Conference on Microwave, Antenna and Remote Sensing (ICMARS-12), 11 - 15 December 2012, ICRS- Jodhpur.

Gupta M., A. Sharma and B. Kartikeyan (2013). RISAT-1 Point Target Analysis Augmented Software Tool. Technical Report: SAC/SIPA/SPDCG/IAQD/RISAT-1/TN-93/Dec.-2013, Space Applications Centre, Ahmedabad.

Gupta M., B. Kartikeyan and S. Chowdhury (2014). An approach to evaluate and monitor RISAT-1 SAR from level-0 raw data. International Journal of Remote Sensing, http://dx.doi.org/10.1080/01431161.2014.943323.

Holm, S., P. Valand, and K. Eldhuset (1991). Performance of CESAR ERS-1 SAR processor. In IGARSS 91, pp. 291 – 294.

Lu, X. and H. Sun (2007). Parameter assessment for SAR image quality evaluation system. In Proc. 1st Asian and Pacific Conf. Synthetic Aperture Radar APSAR 2007, pp. 58–60.

Meadows, P. and P. Wright (2002). ASAR IMP image quality (VV Polarization). Proc. of the ENVISAT calibration review, ESA SP-520, 2002. https://earth.esa.int/calval/proceedings/asar/asar13.pdf.

Mehra R., A. Garg, K. Padia, S. Chowdhury (2013). Approach for generation of RISAT-1 SAR calibrated data products. Technical Report: SAC/SIPA/DPSG/AIPD/RISAT-1 DP/TN-02/April, 2013, Space Applications Centre, Ahmedabad.

Mehta K.B., A.K. Shukla, S. Mohan, K.M. Sreejith and Ajai (2011). Methodology for calibration of ENVISAT - ASAR using triangular trihedral corner reflectors. International Journal of Earth science & Engineering (IJEE), 4, No. 4, 614-622.

Norris, J., P.W. Vachon, D. Schlingmeier, R. English and L. Gallop (2004). Expendable trihedral corner reflectors for target enhancement and position control in RADARSAT-1 fine beam mode SAR imagery: Results from an exercise Narwhal Pre-Trial Deployment Defence R&D Canada-Ottawa TECHNICAL MEMORANDUM DRDC Ottawa TM 2004-197 September 2004.

Prakash S., M. Gupta, B. Kartikeyan (2012). Point target analysis for RISAT-1 SLC data products using corner reflectors. International Conference on Microwave, Antenna and Remote Sensing (ICMARS-12), 11 – 15 December, 2012, ICRS- Jodhpur.

Sanchez, J. (1991). Software tools for quality measurement in SAR images, ESA-ESTEC-X-853, 1991.

Sharma, A., M. Gupta and B. Kartikeyan (2013). RISAT-1 SAR radiometric data quality evaluation using extended target. In International Experts Meet on Microwave Remote Sensing, IEEE-GRSS Gujarat Chapter, 16 – 17 December, Ahmedabad.

Skolnik, M. I. (1990), Radar handbook (2nd ed.), Mc Graw Hill, ISBN 0-07-057913-X, New York, USA

Ulaby, F.T., R.K. Moore and A.K. Fung (1981). Microwave remote sensing; Active and passive, Volume 1, Microwave Remote Sensing: Fundamentals and Radiometry, Addison Wesley Publication Massachusetts, USA